

RSC Advances



This is an *Accepted Manuscript*, which has been through the Royal Society of Chemistry peer review process and has been accepted for publication.

Accepted Manuscripts are published online shortly after acceptance, before technical editing, formatting and proof reading. Using this free service, authors can make their results available to the community, in citable form, before we publish the edited article. This *Accepted Manuscript* will be replaced by the edited, formatted and paginated article as soon as this is available.

You can find more information about *Accepted Manuscripts* in the [Information for Authors](#).

Please note that technical editing may introduce minor changes to the text and/or graphics, which may alter content. The journal's standard [Terms & Conditions](#) and the [Ethical guidelines](#) still apply. In no event shall the Royal Society of Chemistry be held responsible for any errors or omissions in this *Accepted Manuscript* or any consequences arising from the use of any information it contains.

**The facile preparation of novel magnetic zirconia composites
with the aid of carboxymethyl chitosan and their efficient
removal of Dye**

Taiheng Wu, Qian Shao^{*}, Shengsong Ge, Liwei Bao and Qingyun Liu

*College of Chemical and Environmental Engineering, Shandong University of Science
& Technology, Qingdao 266590, China*

E-mail: wutaiheng@126.com

Tel&Fax.: +86 0532 80681197

Abstract:

The novel composites based on magnetic Zirconia was synthesized with the aid of Carboxymethyl Chitosan ($\text{Fe}_3\text{O}_4/\text{ZrO}_2\text{-CMCS}$) by a facile method. The as-synthesized products were characterized by wide-angle powder X-ray diffraction (XRD), scanning electron microscopy (SEM), Fourier transform infrared spectroscopy (FTIR). The Magnetic Zirconia Carboxymethyl Chitosan ($\text{Fe}_3\text{O}_4/\text{ZrO}_2\text{-CMCS}$) composites consisted of particles which show a better regularity and uniform with 200-300 nm in diameter. The as-obtained $\text{Fe}_3\text{O}_4/\text{ZrO}_2\text{-CMCS}$ nanocomposites exhibited high adsorption activity and the adsorption capacity for sunset yellow was up to 143.2 mg/g without adjusting pH of the solution. Interestingly, after the carboxymethyl chitosan being eliminated by calcining in air, the as-obtained $\text{Fe}_3\text{O}_4/\text{ZrO}_2$ showed enhanced photocatalytic activity under sunlight irradiation. The degradation rate of Rhodamine B as well as sunset yellow was 89 % and 84 % in 240 min, respectively, due to the addition of the $\text{Fe}_3\text{O}_4/\text{ZrO}_2$ photocatalyst under sunlight irradiation. Both $\text{Fe}_3\text{O}_4/\text{ZrO}_2\text{-CMCS}$ and $\text{Fe}_3\text{O}_4/\text{ZrO}_2$ can be recycled and reused easily, due to magnetism of iron oxide in the composites. Considering the high adsorption performance of $\text{Fe}_3\text{O}_4/\text{ZrO}_2\text{-CMCS}$ and the enhanced photocatalytic activity of $\text{Fe}_3\text{O}_4/\text{ZrO}_2$ for dye stuff, these two nanocomposites can be applied in treating the waste water contaminated by organic dye stuff.

Keywords: chitosan; ZrO_2 ; Fe_3O_4 ; adsorbent; photocatalyst

1. Introduction

Dye contaminants widely exist in wastewaters discharged by many industries, such as textile, leather, food and paper ^[1]. Due to their toxicity and possible carcinogenicity and mutagenicity, it is necessary and indispensable to remove the dye stuffs from wastewater before they are released into our environment. Adsorbent and photocatalytic degradation technology are expected to play a significant role in solving this issue.

Zirconia (ZrO_2), a chemically inert inorganic metal oxide ^[2], as an n-type semiconductor ^[3], it can be effectively applied as catalysts ^[4,5], catalyst supports ^[6,7], dielectric materials ^[8,9], high-performance ceramic materials ^[10,11], chemical sensors ^[12,13], solid oxide fuel cells ^[14,15], photocatalytic materials ^[16,17], and adsorbent ^[1]. Particularly, as an effective adsorbent, ZrO_2 exhibits a high adsorption capacity and fast adsorption kinetics for environmental remediation due to its high surface area ^[18]. The mesoporous ZrO_2 prepared by Liu et al. ^[19] and the Fe_3O_4 core/mesoporous ZrO_2 shell nanostructures prepared by Sarkar et al. ^[20] both have been used for the adsorption of pollutants from wastewater. However, the adsorption property of a single ZrO_2 adsorbent is still limited by the incompatible characteristic with organic dyes. Therefore, the recombination of ZrO_2 with organic adsorbents causes intense attentions. Chitosan is one of linear copolymer of glucosamine and N-acetyl glucosamine ^[21], the high content of amino and hydroxyl functional groups attached on chitosan macromolecules is essential to adsorb and remove pollutants in water ^[22,23], and it has gained much attention as an effective adsorbent ^[24]. Furthermore,

ZrO₂ adsorbents modified with chitosan will exhibit better adsorption performance than ZrO₂ adsorbents or chitosan adsorbents. For example, CS/Fe₃O₄/ZrO₂ composites reported by Jiang et al.^[1] and CS/MMT/ZrO₂ nanocomposites reported by Teimouri et al.^[25], both exhibited higher adsorption performance and could be used to adsorb dye or pollutants in wastewater.

However, the poor chemical stability and mechanical strength of chitosan^[26] limit its wide application. For example, raw chitosan dissolves in water when the pH of aqueous solution is below 5^[27], so it can only be utilized in acidic waste water. But after chitosan was modified by carboxyl group, the as-obtained derivative of chitosan, carboxymethyl chitosan (CMCS), can significantly solve the limitation of raw chitosan. Because CMCS contains both cations and anions on the backbone chain, it can be dissolved in water over wide pH ranges^[28]. Compared to chitosan, CMCS has more functional group, such as carboxyl, amino and hydroxyl, which makes CMCS more efficient to coordinate metal oxide^[29] and to flocculate sol^[30]. This characteristic is expected to play a pivotal role during the mineralization process like amino-metal coordination and hydrogen bonding between hydroxyl group and oligomeric metal oxide^[31]. If CMCS was combined with ZrO₂, the adsorption properties of ZrO₂/CMCS composites could exhibit better performance. To our best knowledge, there is no report about ZrO₂/CMCS for adsorption removal of organic dyes. To further improve the separation and reutilization, the Fe₃O₄/ZrO₂-CMCS were prepared successfully by a facile precipitation method. And the report on the synthesis of Fe₃O₄/ZrO₂-CMCS composites exhibiting high adsorption activity is not found up

to now. Compared with $\text{Fe}_3\text{O}_4/\text{ZrO}_2\text{-CS}$, the as-prepared $\text{Fe}_3\text{O}_4/\text{ZrO}_2\text{-CMCS}$ composites exhibit a high adsorption capacity for sunset yellow in a wide range of pH. Interestingly, after eliminating the CMCS in the $\text{Fe}_3\text{O}_4/\text{ZrO}_2\text{-CMCS}$ composites through a simple heat treatment, the as-obtained $\text{Fe}_3\text{O}_4/\text{ZrO}_2$ powders displayed a higher photocatalytic activity in degrading dye stuff (Rh B) under sunlight irradiation. Although there have been many reports about ZrO_2 as photocatalyst^[32,33], the $\text{Fe}_3\text{O}_4/\text{ZrO}_2$ composites as photocatalyst prepared by this method have not yet been explored. And with the aid of Fe_3O_4 , $\text{Fe}_3\text{O}_4/\text{ZrO}_2$ composites become more sensitive to visible light than pure ZrO_2 powders alone. Furthermore, both $\text{Fe}_3\text{O}_4/\text{ZrO}_2\text{-CMCS}$ and $\text{Fe}_3\text{O}_4/\text{ZrO}_2$ can be recycled and reused easily due to the presence of the magnetic Fe_3O_4 in the composites.

2. Experimental

2.1. Materials

Chitosan (degree of deacetylation: 99 %; average molecular weight: 200 kD) was purchased from Aladdin Co.. $\text{ZrOCl}_2 \cdot 8\text{H}_2\text{O}$, monochloro acetic acid, glacial acetic acid, ferric chloride, ferrous chloride, sodium hydroxide, hydrochloric acid and absolute ethyl alcohol were purchased from Kermel reagent Co. and used without any other purification.

2.2. Characterization

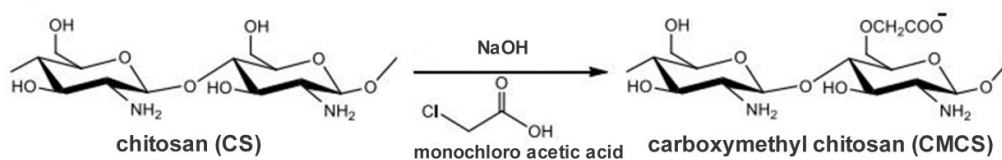
The phase of the as-prepared samples was determined by a Rigaku D/Max 2400 X-ray diffractometer (XRD) equipped with graphite monochromatized $\text{CuK}\alpha$

radiation (30 kV, 100 mA). Fourier transform infrared (FT-IR) spectra were recorded on a NICOLET 380 FT-IR spectrometer (Nicolet Thermo, USA) using a KBr disk method. The morphologies of the samples were imaged by a transmission electron microscope (TEM, FEI Tecnai F30) operated at an accelerating voltage of 300 kV and scanning electron microscope (SEM, JEOL JSM-5600LV). The diffuse reflectance UV-visible spectrum of $\text{Fe}_3\text{O}_4/\text{ZrO}_2$ was recorded on a Cary 100 UV-visible spectrophotometer (Japan, Hitachi, U-3010).

2.3. Synthesis of Fe_3O_4 -CMCS composite

Fe_3O_4 was prepared according to the previous publication [29].

Chitosan was dealt with NaOH according to the following procedure (Scheme 1). In a typical procedure, 3 g of chitosan was dispersed in NaOH solution (50 wt%) and alkalified for 3 hours. Afterward, 15 g of monochloro acetic acid was added into the above mixture under stirring at 90 °C for 30 min. completely, the final mixture was neutralized with glacial acetic acid. The carboxymethyl chitosan was obtained and dried at 50 °C in the air.



Scheme.1. Schematic diagram of chemical reaction of chitosan modified with carboxylic groups.

Preparation of Fe_3O_4 -CMCS is as follows. 1.0 g of as-obtained Fe_3O_4 particles was ultrasonically dispersed into 30 mL of distilled water, followed by mixing with aqueous solution of carboxymethyl chitosan (5.0 g/100 mL) after ultrasonic treatment

for 30 min to form sol of Fe_3O_4 . And the mixture had been stirred for another 6 hours at room temperature. Once the flocculation of Fe_3O_4 -CMCS has formed, the Fe_3O_4 -CMCS would not dissolve in the solution. Then the as-obtained Fe_3O_4 -CMCS was collected with a magnet and washed with distilled water for several times.

2.4. Synthesis of $\text{Fe}_3\text{O}_4/\text{ZrO}_2$ -CMCS and $\text{Fe}_3\text{O}_4/\text{ZrO}_2$ composite

The $\text{ZrOCl}_2 \cdot 8\text{H}_2\text{O}$ solution (0.1 mol/L) was added drop wise into the above mixture of Fe_3O_4 -CMCS until no more precipitation formed. The $\text{Fe}_3\text{O}_4/\text{ZrO}_2$ -CMCS precipitation was collected with a magnet and washed with distilled water for several times. Similarly, $\text{Fe}_3\text{O}_4/\text{ZrO}_2$ -CS was prepared by the similar method except that the chitosan was dissolved into 2 % (V/V) acetic acid.

The $\text{Fe}_3\text{O}_4/\text{ZrO}_2$ composites were obtained by calcining the as-prepared $\text{Fe}_3\text{O}_4/\text{ZrO}_2$ -CMCS at 350 °C in air for 3 hour with a heating rate of 2 °C /min. Similarly, the ZrO_2 powders were prepared by the same method in the absence of Fe_3O_4 .

2.5. Adsorption experiments

10 mg of $\text{Fe}_3\text{O}_4/\text{ZrO}_2$ -CMCS and 50 mL of sunset yellow solution (initial concentration was 100 mg/L) were added in a beaker. After stirring at 25 °C for 60 min, the suspension was separated by a magnet and the supernatant liquid was taken to study the adsorption of sunset yellow. And 0.1 mol/L HCl aqueous solution was used to regenerate the adsorbents which was found to be effective in desorbing sunset yellow from the loaded adsorbents. The reusability experiments were carried out in sunset yellow solution without adjusting the pH (pH=6).

The standard curve of sunset yellow was obtained by measuring the absorbance of sunset yellow solution with different concentration. The equation of standard curve was as following:

$$A = 0.00936 + 0.02768 \times c_{\text{eq}}, R^2 = 0.9999 \quad (1)$$

On the basis of Eq.(1), the adsorbing capacity (Q_e (mg.g⁻¹)) was calculated as following:

$$Q_e = (c_0 - c_{\text{eq}}) \times V / W \quad (2)$$

Where A is the absorbance; c_{eq} is the equilibrium concentration of sunset yellow (mg/L); R is the correlation coefficient; c_0 is the initial concentration of sunset yellow (mg/L); V is the volume of the experimental solution (L); and W is the weight of adsorbent (g).

2.6. Photocatalytic experiments

50 mg of Fe₃O₄/ZrO₂ was dispersed in 50 mL of Rhodamine B aqueous solution (10 mg/L, pH = 8). After being stirred in the dark for 60 min to reach adsorption equilibrium, the mixture was transferred to the photochemical reactor under irradiation of sun-light (Xe lamp 245 W).

3. Results and discussions

3.1. Characterization of Fe₃O₄/ZrO₂-CMCS and Fe₃O₄/ZrO₂

XRD patterns of the Fe₃O₄/ZrO₂-CMCS and Fe₃O₄/ZrO₂ samples are presented in Fig. 1. In Fig. 1A, the peak at 31.15°, 35.27°, 43.32°, 53.64° 57.13° and 62.29° can be assigned to Fe₃O₄ (JCPDS Card No.26-1136). The peak at 30.13°, 35.03°, 50.27°

and 60.08° can be assigned to ZrO_2 (JCPDS Card No. 02-0733). Meanwhile, because of the poor crystallinity of carboxymethyl chitosan, only a broad peak at about 20° - 40° is appeared due to hydrogen bonds of carboxymethyl chitosan. After being heated at 350°C for 1h, the diffraction peaks of $\text{Fe}_3\text{O}_4/\text{ZrO}_2$ can be observed clearly in Fig. 1B. The characteristic peaks at 30.51° , 35.65° , 50.74° , 60.11° and 63.88° are from the (111), (200), (220), (311) and (222) crystal planes of the tetragonal ZrO_2 [34] (JCPDS Card No. 02-0733). It can be also found that peaks at 2θ of 31.53° , 33.14° , 45.35° , 54.54° , 57.48° and 62.40° are corresponding to (220), (311), (400), (422), (511) and (440) reflections of the inverse spinel structure of Fe_3O_4 (JCPDS Card No. 26-1136). No additional peaks can be observed. The data of XRD, shown in Fig. 1B, indicates that carboxymethyl chitosan from the composites has been decomposed completely and the as-prepared $\text{Fe}_3\text{O}_4/\text{ZrO}_2$ particles show better degree of crystallinity without carboxymethyl chitosan. From Fig. 1A, it can be seen that the diffraction peaks of $\text{Fe}_3\text{O}_4/\text{ZrO}_2$ -CMCS are slightly broadened because of the smaller crystallite size than that of $\text{Fe}_3\text{O}_4/\text{ZrO}_2$ (Fig. 1B). This result was further confirmed by the SEM image, shown in Fig. 2A and Fig. 2C. The phase structure of as-prepared ZrO_2 was examined by XRD as well. As shown in Fig. 1C, no characteristic peaks from other crystalline impurities were detected by XRD, thereby suggesting that all samples were purity ZrO_2 .

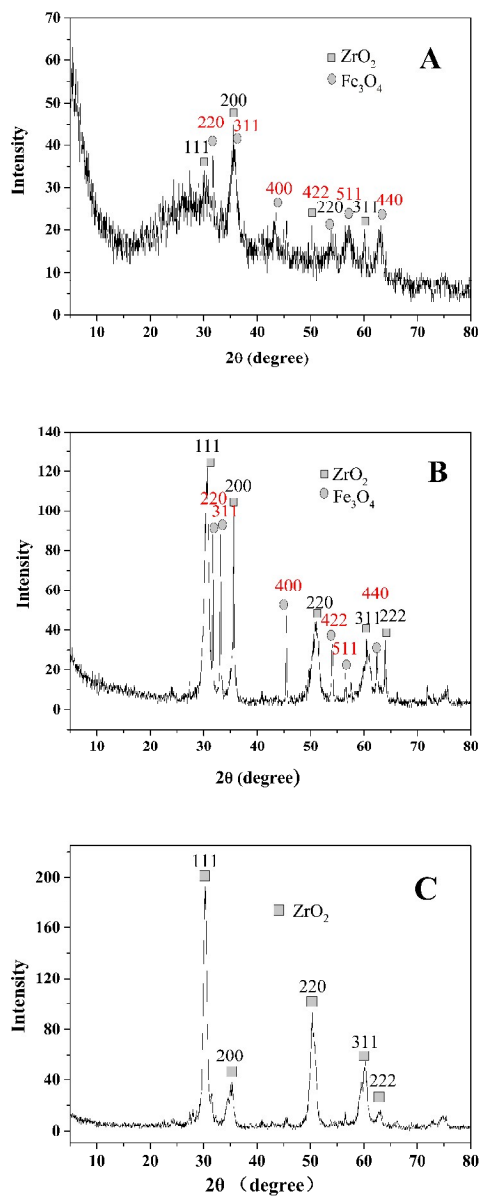


Fig.1. XRD patterns of the Fe₃O₄/ZrO₂-CMCS (A), Fe₃O₄/ZrO₂ (B), and ZrO₂ (C).

The morphologies of the as-prepared Fe₃O₄/ZrO₂-CMCS and Fe₃O₄/ZrO₂ are imaged by SEM and TEM, respectively. From Fig.2A, and 2B, it can be observed clearly that the agglomerated particle of synthesized Fe₃O₄/ZrO₂-CMCS consists of particles with the diameter of 200-300 nm, which is similar to the coral rock that

zirconium oxide and iron oxide deposited on the line-agglomerated chitosan. On the whole, the $\text{Fe}_3\text{O}_4/\text{ZrO}_2\text{-CMCS}$ has no uniform morphology as titania-chitosan and titanium hydrate-chitosan template reported in the previous publications^[35,36]. Fig. 2C shows the image of the obtained $\text{Fe}_3\text{O}_4/\text{ZrO}_2$ particles after calcining the $\text{Fe}_3\text{O}_4/\text{ZrO}_2\text{-CMCS}$ composites at 350 °C. Compared with $\text{Fe}_3\text{O}_4/\text{ZrO}_2\text{-CMCS}$, the particle size of $\text{Fe}_3\text{O}_4/\text{ZrO}_2$ become bigger but not change significantly (may be due to the agglomeration effect). And the dispersity of particles has been improved obviously due to disappearance of the media of chitosan. Furthermore, the image of ZrO_2 powders using the same method in the absence of Fe_3O_4 is shown in Fig. 2D. The morphology of ZrO_2 is agglomerated cube without uniform shape, but the particle size is smaller compared with $\text{Fe}_3\text{O}_4/\text{ZrO}_2$.

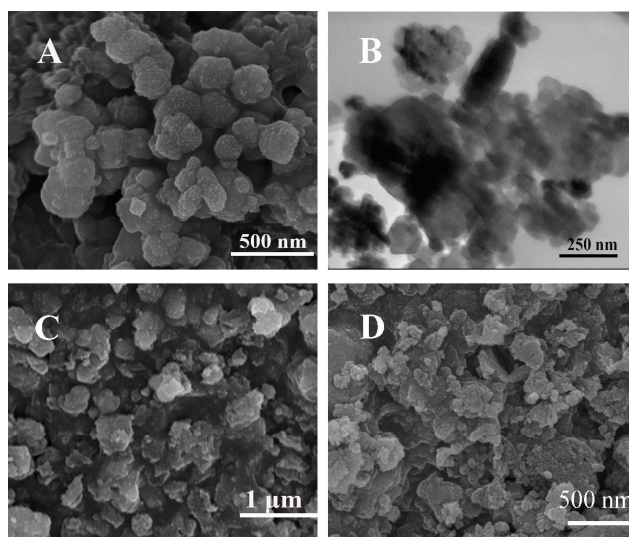


Fig.2 SEM (A) and TEM (B) images of $\text{Fe}_3\text{O}_4/\text{ZrO}_2\text{-CMCS}$, SEM (C) image of $\text{Fe}_3\text{O}_4/\text{ZrO}_2$ and SEM (D) image of ZrO_2 .

Fig. 3 shows the FT-IR spectra of the chitosan (a), $\text{Fe}_3\text{O}_4/\text{ZrO}_2\text{-CMCS}$ (b) and

$\text{Fe}_3\text{O}_4/\text{ZrO}_2$ (c), respectively. From Fig. 3b, it can be seen that the FT-IR spectrum of $\text{Fe}_3\text{O}_4/\text{ZrO}_2\text{-CMCS}$ shows predominant peaks at 1600 cm^{-1} and 3450 cm^{-1} , assigned to the N-H bending vibration and O-H stretching vibration of carboxymethyl chitosan, respectively. The peak at 1400 cm^{-1} is related to the $-\text{COOH}$ bending vibration. The sharp peak at 455 cm^{-1} is corresponding to the Zr-O vibrations, while the peak at 559 cm^{-1} is attributed to the Fe-O vibrations. From Fig. 3b, it can be seen that the peak at 3450 cm^{-1} and $\sim 1600\text{ cm}^{-1}$ are decreased while the peak at 1400 cm^{-1} is enhanced, owing to the coordination interaction between metal atoms and amino as well as reaction between $-\text{OH}$ and chloroacetic acid. The coordination interaction is also confirmed by the vibration at 455 cm^{-1} and 559 cm^{-1} attributed to Zr-O and Fe-O vibrations (Fig. 3b and 3c), respectively.

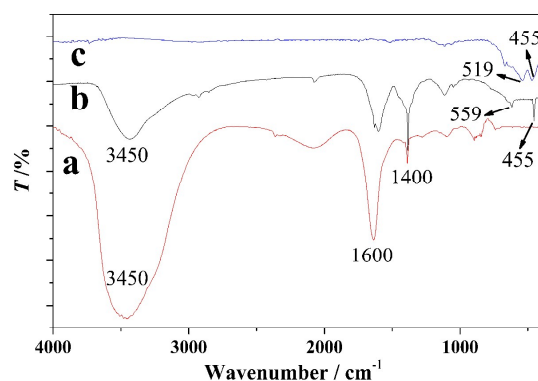


Fig.3. FTIR spectra of the chitosan (a), $\text{Fe}_3\text{O}_4/\text{ZrO}_2\text{-CMCS}$ (b) and $\text{Fe}_3\text{O}_4/\text{ZrO}_2$ (c).

3.2. Formation mechanism

From the observed XRD, SEM and FTIR results, the possible pathway for the formation of the $\text{Fe}_3\text{O}_4/\text{ZrO}_2\text{-CMCS}$ and $\text{Fe}_3\text{O}_4/\text{ZrO}_2$ composites could be predicted.

This mechanism mainly consists of three stages, and the detailed formation progress is described as following: In the first step, when the aqueous solution of CMCS was mixed with the sol of Fe_3O_4 , as a linear polymer, CMCS could flocculate the sol of Fe_3O_4 to form Fe_3O_4 -CMCS composites by means of bridging effect^[37] and charge neutralization effect^[28]. In the second step, when the $\text{ZrOCl}_2 \cdot 8\text{H}_2\text{O}$ solution was added drop wise into the mixture of Fe_3O_4 -CMCS, the zirconium (IV) chloride would gradually hydrolyze and the hydrous zirconia containing OH groups would be coordinated by the amino groups on the surface of CMCS^[38,39] gradually to form $\text{Fe}_3\text{O}_4/\text{ZrO}_2$ -CMCS composites. Moreover, the hydrogen bonding between hydroxyl group on the surface of CMCS and hydrous zirconia also plays a pivotal role in this step. Finally, after calcining in air, CMCS was eliminated and condensation reaction between zirconium hydroxide and surplus OH surrounding Fe_3O_4 ^[40] occurred to form $\text{Fe}_3\text{O}_4/\text{ZrO}_2$ composites.

3.3. Adsorption activity

The removal of dyes in containing waste water is an urgent question to solve. Various physical and chemical methods are used efficiently. Adsorption technique is generally used to removal dyes in containing water. At present, adsorption techniques appears to be a feasible option technically and economically, so there has been increased interest in the use of other adsorbent materials, particularly low-cost adsorbents. Sunset yellow is a pyrazolone dye used in common food products such as beverages, candies, dairy products, pharmaceuticals and bakery products. Hence,

Sunset yellow is selected as a model reactant to evaluate the adsorption activity of the $\text{Fe}_3\text{O}_4/\text{ZrO}_2\text{-CMCS}$ composites.

Table.1. Comparison of sunset yellow adsorption capacity of $\text{Fe}_3\text{O}_4/\text{ZrO}_2\text{-CMCS}$, $\text{Fe}_3\text{O}_4/\text{ZrO}_2\text{-CS}$,

$\text{Fe}_3\text{O}_4\text{-CMCS}$ and CS with different pH.

$\text{Fe}_3\text{O}_4/\text{ZrO}_2\text{-CMCS}$	pH	1.92	2.80	4.89	7.59	10.73	11.80
	$Q_e/\text{mg.g}^{-1}$	155.97	138.32	115.37	129.12	101.57	4.39
$\text{Fe}_3\text{O}_4/\text{ZrO}_2\text{-CS}$	pH	2.78	3.74	5.27	7.02	10.98	11.93
	$Q_e/\text{mg.g}^{-1}$	134.69	99.39	82.71	86.46	42.22	1.21
$\text{Fe}_3\text{O}_4\text{-CMCS}$	pH	1.93	2.82	3.28	5.99	8.91	11.20
	$Q_e/\text{mg.g}^{-1}$	213.87	177.86	122.86	25.94	1.28	0.91
CS	pH	2.34	3.97	5.01	6.74	9.79	11.03
	$Q_e/\text{mg.g}^{-1}$	66.24	40.75	28.97	14.38	1.02	0.63

Table.1 and Fig.4 show that $\text{Fe}_3\text{O}_4/\text{ZrO}_2\text{-CMCS}$ as an adsorbent demonstrates a high adsorption capacity in broad range of pH (pH=3~10). Although it seems that $\text{Fe}_3\text{O}_4\text{-CMCS}$ has higher adsorption capacity than $\text{Fe}_3\text{O}_4/\text{ZrO}_2\text{-CMCS}$ at low pH (< 2.8), the adsorption capacity of $\text{Fe}_3\text{O}_4\text{-CMCS}$ decreases significantly when pH>3. After ZrO_2 is composited in the adsorbent, $\text{Fe}_3\text{O}_4/\text{ZrO}_2\text{-CMCS}$ demonstrates a high and stable adsorption capacity in broad range of pH (pH=3~10) compared with $\text{Fe}_3\text{O}_4\text{-CMCS}$. Meanwhile, compared with $\text{Fe}_3\text{O}_4/\text{ZrO}_2\text{-CS}$ and CS, the adsorption capacity of $\text{Fe}_3\text{O}_4/\text{ZrO}_2\text{-CMCS}$ was significantly improved. It is possible because that CMCS exhibits higher concentration of active sites than CS, which makes it possible

to not only offer enough adsorption groups for increasing adsorption capacity [29,30] toward dye but also improve the flocculation capacity for dye molecules [41]. Furthermore, the adsorption ability also increases with increasing molecular weight of the polymer [42,43].

However, the adsorption capacity of $\text{Fe}_3\text{O}_4/\text{ZrO}_2\text{-CMCS}$ decreases significantly when pH is more than 10. At lower pH, the high adsorption capacity is mainly due to the strong electrostatic interaction and the positively charged sites of the composite, because amino groups attached with carboxymethyl chitosan and hydroxyl groups attached with ZrO_2 are easily protonated to form positive group in acidic solution [44,45]. But with increasing of pH, the surfaces of the composites gradually become negative (the isoelectric points of chitosan and ZrO_2 are at $\text{pH} = 6.4$ [44] and $\text{pH} = 5.7$ [45], respectively). So the electrostatic interaction between the anions and the adsorbent becomes so weak that it is negligible which lead to the adsorption capacity gradually decreases.

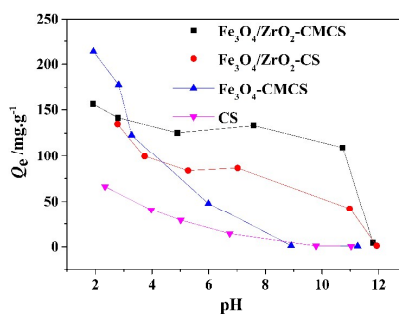


Fig.4. Comparison of sunset yellow adsorption capacity of $\text{Fe}_3\text{O}_4/\text{ZrO}_2\text{-CMCS}$, $\text{Fe}_3\text{O}_4/\text{ZrO}_2\text{-CS}$, $\text{Fe}_3\text{O}_4\text{-CMCS}$, CS with different pH.

The effects of adsorption time and reusability were investigated in sunset yellow

solution without adjusting pH (pH=6). In Fig.5A, it is apparent that there are two stages in the process of reaction. In the initial stage, the high rate of adsorption is probably due to a large amount of binding sites on the surface of $\text{Fe}_3\text{O}_4/\text{ZrO}_2\text{-CMCS}$. In the second stage, the rate of adsorption becomes slower until the adsorption equilibrium is reached. The result demonstrates that $\text{Fe}_3\text{O}_4/\text{ZrO}_2\text{-CMCS}$ can adsorb sunset yellow quickly and the adsorption equilibrium can reach within ~40 min. The maximal adsorption capacity is up to 143.2 mg/g.

The $\text{Fe}_3\text{O}_4/\text{ZrO}_2\text{-CMCS}$ adsorbent can be collected easily by a magnet, due to adding of magnetic Fe_3O_4 in the composites. In the first trial, the adsorption capacity of sunset yellow was 143.2 mg/g. Moreover, in succeeding six recycles for the adsorption of sunset yellow, the $\text{Fe}_3\text{O}_4/\text{ZrO}_2\text{-CMCS}$ still maintained a relative higher adsorption capacity. These results indicated no appreciable loss in activity over at least five cycles. And the data of reusability experiment was shown in Fig.5B.

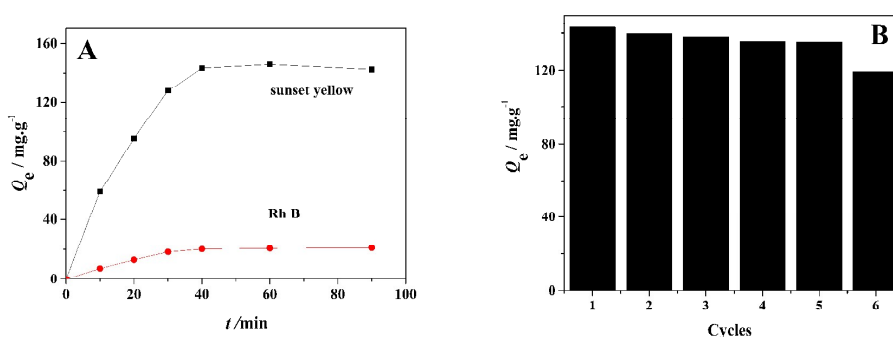


Fig.5. Effects of adsorption time (A) reusability (B) on the adsorption capacities of

$\text{Fe}_3\text{O}_4/\text{ZrO}_2\text{-CMCS}$

3.4. Photocatalytic activity

Some kinds of dye stuff in waste water could be removed not only by adding of adsorbents but also by adding of photocatalyst. Based on the above results (as shown in Fig.5A), the adsorption capacity of Fe₃O₄/ZrO₂-CMCS for sunset yellow was up to 143.2 mg/g, while it was only 20.07 mg/g for Rhodamine B. However, Fe₃O₄/ZrO₂ has great photocatalytic efficiency for dye stuff in contaminated water. Thus, after the carboxymethyl chitosan being eliminated by calcining in air, the as-obtained Fe₃O₄/ZrO₂ powders as photocatalyst were used to remove Rhodamine B.

Fig. 6A shows the UV-vis absorption spectra of the Fe₃O₄/ZrO₂ composites. From Fig. 6A, the band gap of the Fe₃O₄/ZrO₂ composites can be obtained. The equation $(Ah\nu)^2 = K(h\nu - E_g)$ was used to calculate the band gap, where A is the absorption coefficient, K is a proportionality constant, and E_g is the band-gap energy. The plotting of $(Ah\nu)^2$ vs. $h\nu$ based on the direct transition is shown in Fig. 6B. The absorption edge of pure ZrO₂ powders is observed at ~360 nm, corresponding to the band gap energy of 3.0 eV. Compared with pure ZrO₂ powders, the absorption intensity of the Fe₃O₄/ZrO₂ powders is obviously increased in the visible light region, corresponding to the band gap energy of 2.5 eV. These results reveal that the Fe₃O₄/ZrO₂ composites are more sensitive to visible light than pure ZrO₂ powders alone. Therefore, the as-prepared Fe₃O₄/ZrO₂ composites are expected to demonstrate enhanced photocatalytic activity under sunlight irradiation.

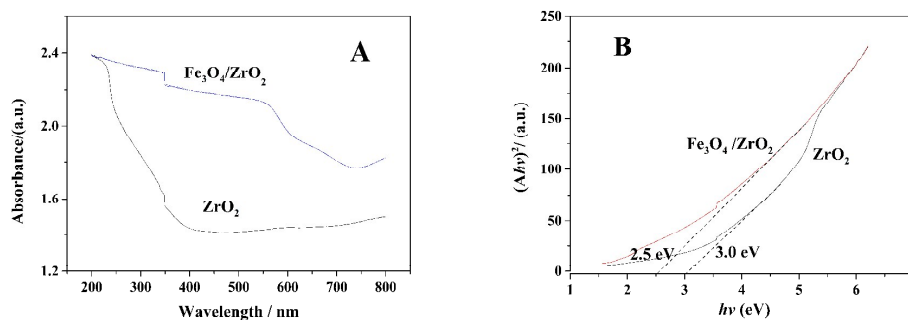


Fig.6. UV-visible spectra of the as-prepared ZrO_2 and $\text{Fe}_3\text{O}_4/\text{ZrO}_2$ powders (A) and The plotting of $(A/h\nu)^2$ vs $h\nu$ based on the direct transition (B).

The photocatalytic activity of $\text{Fe}_3\text{O}_4/\text{ZrO}_2$ composites has been evaluated by the degradation of Rh B under sunlight. Comparative experiments were carried out in the presence of the as-prepared $\text{Fe}_3\text{O}_4/\text{ZrO}_2$ catalysts or in the absence of $\text{Fe}_3\text{O}_4/\text{ZrO}_2$ catalysts. Initial pH is vital experimental parameters. From Fig.7 shown, when the initial concentration of Rh B is 10 mg/L, and the amount of $\text{Fe}_3\text{O}_4/\text{ZrO}_2$ catalyst is 1 g/L, with increasing the pH until reaching the optimum value (pH=8), the reaction rate of Rh B photodegradation were observed to increase. At a higher pH of RhB, the photodegradation rate decreased.

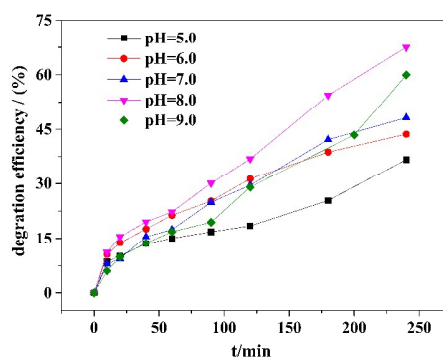


Fig.7. Effect of pH on the degradation efficiency of Rh B.

From Fig. 8A, it can be seen that the absorbance of Rh B solution gradually decreased with the extension of experimental time using the as-synthesized $\text{Fe}_3\text{O}_4/\text{ZrO}_2$ as catalysts. Moreover, the degradation of sunset yellow was also examined as shown in Fig. 8B. The degradation rate of Rh B and sunset yellow were more than 89 % and 84 % under the sun light in 240 min using $\text{Fe}_3\text{O}_4/\text{ZrO}_2$ powders as photocatalyst, while it is only 68 % and 14 % using ZrO_2 as photocatalyst and without photocatalyst under the same experimental conditions, respectively, as shown in Fig. 8C.

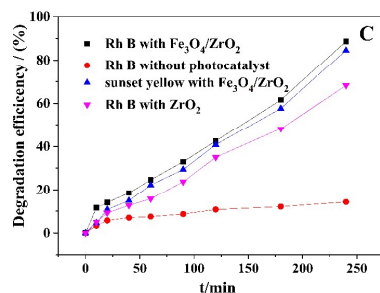
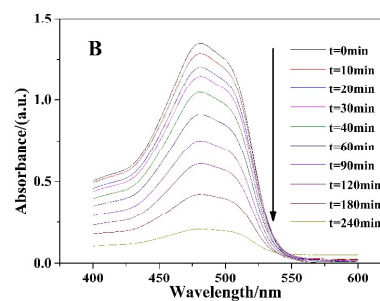
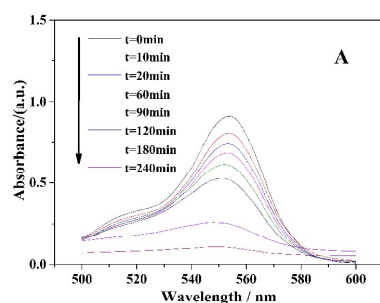


Fig.8. The UV-vis absorption spectra of Rh B solution (A) and sunset yellow solution (B) using $\text{Fe}_3\text{O}_4/\text{ZrO}_2$ powders as catalysts in different time; The degradation efficiency at different irradiation times (C).

4. Conclusion

In summary, the $\text{Fe}_3\text{O}_4/\text{ZrO}_2$ -CMCS composite was synthesized with the aid of modified chitosan by introducing carboxylic groups. The $\text{Fe}_3\text{O}_4/\text{ZrO}_2$ -CMCS exhibits excellent adsorption activity for sunset yellow. Moreover, after removal of chitosan from the $\text{Fe}_3\text{O}_4/\text{ZrO}_2$ -CMCS composites, the obtained $\text{Fe}_3\text{O}_4/\text{ZrO}_2$ inorganic composites demonstrate a high photocatalytic activity for the degradation of dye stuff, such as Rh B and sunset yellow under sunlight irradiations. Both as-prepared $\text{Fe}_3\text{O}_4/\text{ZrO}_2$ -CMCS and $\text{Fe}_3\text{O}_4/\text{ZrO}_2$ composites might have potential industrial applications in the environmental field.

Acknowledgment

This work was financially supported by the National Natural Science Foundation of China (Grant No.21271119).

References

- [1] H. L. Jiang, P. H. Chen, S. L. Luo, et al., *J. Inorg. Organomet* p. 23 (2013) 393.
- [2] L. Kljajevic, B. Matovic, A. Radosavljevic-Mihajlovi c, et al., *J. Alloys. Compd.* 509 (2011) 2203.

- [3] M. Labaki, H. Laversin, E. A. Zhilinskaya, et al., *Catal. Commun.* 17 (2012) 64.
- [4] E. I. Kauppi, E. H. Rönkkönen, S. M. K. Airaksinen, et al., *Appl. Catal. B: Environ.* 111-112 (2012) 605.
- [5] M. Labaki, H. Laversin, E. A. Zhilinskaya, et al., *Catal. Commun.* 17 (2012) 64.
- [6] X. Zhang, H. Su, X. Yang, *J. Mol. Catal. A: Chem.* 360 (2012) 16.
- [7] M. Signoretto, F. Menegazzo, L. Contessotto, et al., *Appl. Catal. B: Environ.* 129 (2013) 287.
- [8] W. Zhang, Y. Cui, Z. G. Hu, et al., *Thin. Solid. Films.* 520 (2012) 6361.
- [9] O. Bethge, C. Henkel, S. Abermann, et al., *Appl. Surf. Sci.* 258 (2012) 3444.
- [10] P. P. Shukla, J. Lawrence, *Opt. Laser. Technol.* 43 (2011) 1292.
- [11] Y. Wang, J. Liu, A. Guo, *ceramics, Ceram. Int.* 39 (2013) 883.
- [12] T. Liu, L. Li, J. Yu, *Sens. Actuators. B: Chem.* 139 (2009) 501.
- [13] R. Zhang, X. Zhang, S. Hu, *Sens. Actuators. B: Chem.* 149 (2010) 143.
- [14] H. J. Cho, G. M. Choi, *J. Power. Sources.* 176 (2008) 96.
- [15] W. Sun, N. Zhang, Y. Mao, *J. Power Sources.* 218 (2012) 352.
- [16] A. A. Ashkarran, S. A. A. Afshar, S. M. Aghigh, *Polyhedron.* 29 (2010) 1370.
- [17] A. B. Nawale, N. S. Kanhe, S. V. Bhoraskar, et al., *Mater. Res. Bull.* 47 (2012) 3432.
- [18] P. Wang, I. M. C. Lo, *Water Res.* 43 (2009) 3727.
- [19] H. Liu, X. Sun, C. Yin, C. Hu, et al. *J. Hazard. Mater.* 151 (2008) 616.
- [20] A. Sarkar, S.K. Biswas, P. Pramanik, *J. Mater. Chem.* 20 (2010) 4417.
- [21] G. Y. Li, Y. R. Jiang, K. L. Huang, et al., *J. Alloys. Compd.* 466 (2008) 451.
- [22] A. Bhatnagar, M. Sillanpää, *J. Chem. Eng.* 168 (2010) 493.
- [23] M. A. Salam, M. S. I. Makki, M. Y. A. Abdelaal, et al., *J. Alloys. Compd.* 509 (2011) 2582.

- [24] Z. E. V. Escobar, P. C. A. Martinez, G. C. A. Rodriguez, et al., *J. Alloys. Compd.* 536 (2012) 441.
- [25] A. Teimouri, S. Ghanavati nasab, S. Habibollahi, et al. *RSC Adv.* 5(9) (2014) 6771.
- [26] E. Guibal, *Sep. Purif. Technol.*, 38 (2004) 43.
- [27] G. Crini, P. M. Badot, *Prog. Polym. Sci.* 33 (2008) 399.
- [28] Z. Yang, B. Yuan, X. Huang, et al., *water res.* 46 (2012) 107.
- [29] L. L. Fan, C. N. Luo, L. Zhen, et al., *Colloid. Surface. B.* 88 (2011) 574.
- [30] G. Crini, *Dyes and Pigments.* 77 (2008) 415.
- [31] E. K. Abdelkrim, M. Karine, C. Thomas, et al., *Microporous. Mesoporous. Mater.* 142 (2011) 301.
- [32] H. Zheng, K. Y. Liu, H. Q. Cao, et al., *J. Phys. Chem. C.* 113 (2009) 18259.
- [33] N. C. S. Selvam, A. Manikandan, L. J. Kennedy, et al., *J. Colloid. Interface. Sci.* 389 (2013) 91.
- [34] J. V. Smith, X-ray Powder Data File, American Society for Testing Materials. (1960).
- [35] T. Preethi, B. Abarna, G. R. Rajarajeswari, *Appl. Surf. Sc.* 317 (2014) 90.
- [36] J. Liu, W. Y. Li, Y. G. Liu, et al., *Appl. Surf. Sc.* 293 (2014) 46.
- [37] F. Renault, B. Sancey, J. Charles, et al., *Chem. Eng. J.* 155 (2009) 775.
- [38] E. Guibal, *Prog. Polym. Sci.* 30 (2005) 71.
- [39] M. Rinaudo, *Prog. Polym. Sci.* 31 (2006) 603.
- [40] H. R. Chen, J. H. Gao, M. L. Ruan, *Micropor. Mesopor. Mat.* 76 (2004) 209.
- [41] L. Wang, A. Q. Wang, *Bioresource Technol.* 99 (2008) 1403–1408.
- [42] J. Blaakmeer, M. R. Böhmer, M. A. Cohen Stuart, et al., *Macromolecules* 23 (1990) 2301.

[43] O. Rustemeier, E. Killmann, J. Colloid Interface Sci. 190 (1997) 360.

[44] S. Chatterjee, S. H. Woo, J. Hazard. Mater. 164 (2009) 1012.

[45] A. Sarkar, S. K. Biswas, P. Pramanik, J. Mater. Chem. 20 (2010) 4417.

The facile preparation of novel magnetic zirconia composites with the aid of carboxymethyl chitosan and their efficient removal of Dye

Taiheng Wu, Qian Shao^{*}, Shengsong Ge, Liwei Bao and Qingyun Liu

College of Chemical and Environmental Engineering, Shandong University of Science & Technology, Qingdao 266590, China

The novel composites based on Magnetic Zirconia was synthesized with the aid of Carboxymethyl Chitosan ($\text{Fe}_3\text{O}_4/\text{ZrO}_2\text{-CMCS}$) by a facile method. The as-obtained $\text{Fe}_3\text{O}_4/\text{ZrO}_2\text{-CMCS}$ nanocomposites exhibited high adsorption activity and the adsorption capacity for sunset yellow was up to 143.2 mg/g without adjusting pH of the solution. Interestingly, after the carboxymethyl chitosan being eliminated by calcining, the as-obtained $\text{Fe}_3\text{O}_4/\text{ZrO}_2$ showed enhanced photocatalytic activity under sunlight irradiation. The degradation rate of Rhodamine B as well as sunset yellow was 89 % and 84 % in 240 min, respectively, due to the addition of the $\text{Fe}_3\text{O}_4/\text{ZrO}_2$ photocatalyst under sunlight irradiation. Both $\text{Fe}_3\text{O}_4/\text{ZrO}_2\text{-CMCS}$ and $\text{Fe}_3\text{O}_4/\text{ZrO}_2$ can be recycled and reused easily, due to magnetism of iron oxide in the composites.

